Biochimica et Biophysica Acta 1840 (2014) 129–135

Contents lists available at ScienceDirect

Biochimica et Biophysica Acta

journal homepage: www.elsevier.com/locate/bbagen

Crystal structures of CbpF complexed with atropine and ipratropium reveal clues for the design of novel antimicrobials against *Streptococcus pneumoniae*

Noella Silva-Martín [a,1], M. Gracia Retamosa [b,2], Beatriz Maestro [b], Sergio G. Bartual [a], María J. Rodes [b], Pedro García [c], Jesús M. Sanz [b,*,3], Juan A. Hermoso [a,*,3]

[a] Departamento de Cristalografía y Biología Estructural, Instituto de Química-Física 'Rocasolano', Consejo Superior de Investigaciones Científicas, Serrano 119, 28006 Madrid, Spain
[b] Instituto de Biología Molecular y Celular, Universidad Miguel Hernández, 03202 Elche, Spain
[c] Centro de Investigaciones Biológicas, Consejo Superior de Investigaciones Científicas, Ramiro de Maeztu, 9, 28040 Madrid, Spain

ARTICLE INFO

Article history:
Received 19 March 2013
Received in revised form 3 September 2013
Accepted 4 September 2013
Available online 11 September 2013

Keywords:
Antibiotic resistance
CBP family
Crystallography
Streptococcus pneumoniae
Atropine
Ipratropium

ABSTRACT

Background: Streptococcus pneumoniae is a major pathogen responsible of important diseases worldwide such as pneumonia and meningitis. An increasing resistance level hampers the use of currently available antibiotics to treat pneumococcal diseases. Consequently, it is desirable to find new targets for the development of novel antimicrobial drugs to treat pneumococcal infections. Surface choline-binding proteins (CBPs) are essential in bacterial physiology and infectivity. In this sense, esters of bicyclic amines (EBAs) such as atropine and ipratropium have been previously described to act as choline analogs and effectively compete with teichoic acids on binding to CBPs, consequently preventing *in vitro* pneumococcal growth, altering cell morphology and reducing cell viability.
Methods: With the aim of gaining a deeper insight into the structural determinants of the strong interaction between CBPs and EBAs, the three-dimensional structures of choline-binding protein F (CbpF), one of the most abundant proteins in the pneumococcal cell wall, complexed with atropine and ipratropium, have been obtained.
Results: The choline analogs bound both to the carboxy-terminal module, involved in cell wall binding, and, unexpectedly, also to the amino-terminal module, that possesses a regulatory role in pneumococcal autolysis.
Conclusions: Analysis of the complexes confirmed the importance of the tropic acid moiety of the EBAs on the strength of the binding, through π–π interactions with aromatic residues in the binding site.
General significance: These results represent the first example describing the molecular basis of the inhibition of CBPs by EBA molecules and pave the way for the development of new generations of antipneumococcal drugs.

1. Introduction

Streptococcus pneumoniae (pneumococcus), a Gram-positive encapsulated diplococcus bacterium, is a major cause of invasive infections (meningitis, bacteremia) and diseases affecting the upper (otitis media and sinusitis) and lower (pneumonia) respiratory tracts, among others [1]. Pneumococcal diseases are widespread both in developed and developing countries with more than 1.6 million deaths per year according to the World Health Organization [2], half of them in children under five [3]. Nowadays, vaccination based on the polysaccharidic capsule, together with treatment with β-lactam antibiotics, currently constitutes the major choices to tackle pneumococcal diseases [1]. However, the wide diversity of *S. pneumoniae* (more than 90 different serotypes) and the increasing emergence of antibiotic-resistant strains make it necessary to search for new methods to fight this microorganism. Therefore, new effective and selective strategies are needed that take into account novel targets common to most pneumococcal isolates.

A characteristic feature of the pneumococcal cell wall is the presence of teichoic acid units decorated with phosphorylcholine residues [4] acting as attachment ligands for the so-called choline-binding proteins (CBPs). The CBP family does not only include proteins from *S. pneumoniae* but also from several of its bacteriophages, as well as from a few other related bacterial species [5–7]. The pneumococcal CBPs are present in all isolates and are essential for the viability and virulence of this microorganism, being involved in processes such as cell-wall division, release of bacterial toxins and adhesion to the host [6–8]. All CBPs share the presence of choline-binding modules (CBMs) (http://pfam.sanger.ac.uk//family/PF01473), which are in turn built up from a variable number of choline-binding repeats (CBRs) of

Abbreviations: CBM, choline-binding module; CBP, choline-binding protein; CBR, choline-binding repeat; CbpF, choline-binding protein F; EBAs, esters of bicyclic amines; DEAE, diethylaminoethyl

* Corresponding authors.
E-mail addresses: jmsanz@umh.es (J.M. Sanz), xjuan@iqfr.csic.es (J.A. Hermoso).
[1] Present address: European Molecular Biology Laboratory (EMBL), Structural and Computational Biology Unit, Heidelberg, Germany.
[2] Present address: Universidad del País Vasco. 20018 San Sebastián, Spain.
[3] These authors contributed equally to this work.

0304-4165/$ – see front matter © 2013 Elsevier B.V. All rights reserved.
http://dx.doi.org/10.1016/j.bbagen.2013.09.006

approximately 20 residues, very rich in aromatic amino acids. So far, the three-dimensional structure of four pneumococcal CBPs has been elucidated, namely Cpl-1 [9], CbpE (also named Pce) [10], CbpF [11] and LytC [12], as well as the isolated CBM modules from the LytA amidase (C-LytA protein) [13] and the Spr1274 protein [14]. The basic CBR is comprised of a 12–14-residue β-hairpin followed by an 8–10-residue loop, conforming a ββ-3-solenoid superhelix. Choline-binding sites in CBPs involve the participation of two aromatic amino acids from one hairpin and another one from the next, configuring a hydrophobic pocket that accommodates the choline methyl groups and establish cation–π interactions with the positive charge of the ligand. Furthermore, a variety of choline analogs such as diethylaminoethanol (DEAE) efficiently emulates the role of choline [15], a characteristic that is commonly used for the single-step purification of CBM-tagged fusion proteins [16,17].

Since CBPs are common to all serotypes, they are attractive drug targets for the treatment of pneumococcal diseases, as their selective inhibition might constitute a promising way for new therapies. In this sense, exogenously added choline and choline analogs have been shown to competitively inhibit the binding of CBPs to the cell wall, blocking cell separation and the characteristic autolysis of *S. pneumoniae* at the end of the stationary phase of growth, and inducing instead the formation of long chains [15,16,18–20]. These effects are also thought to reduce bacterial virulence by preventing the release of toxins upon cell autolysis and limiting the dissemination of the bacteria on the host tissue during infection. Remarkably, esters of bicyclic amines (EBAs) such as atropine and ipratropium (Fig. 1) have proved to be stronger binders than choline and more deleterious at lower concentrations, inducing morphological changes in the cell surface and, more importantly, preventing cell growth in liquid media and decreasing cell viability in more than 90% [21]. Atropine is an alkaloid from *Atropa belladonna*, that is used as a cholinergic blocking drug in premedication for anesthesia and in ophthalmology, and ipratropium is another anticholinergic agent that is employed as antiasthmatic and bronchodilatator. While these EBAs could be thought as potential antimicrobials *per se*, their anticholinergic side-effects may constitute a serious drawback. Instead, they should be considered as head compounds from which new variants can be rationally designed, and to do so, exhaustive, structural information on their interaction with CBPs is needed. In this article we study the structure of crystal complexes between EBAs and CbpF, one of the most abundant choline-binding proteins in the surface of *S. pneumoniae*, and that has been proved to inhibit *in vivo* the autolytic LytC muramidase and to play a direct role in the regulation of pneumococcal autolysis. The results highlight the structural importance of the aromatic rings in the ligands and give clues for the development of new EBA derivatives with antipneumococcal properties.

2. Materials and methods

2.1. Materials

Choline chloride, ipratropium bromide, atropine sulphate and DEAE-cellulose were from Sigma-Aldrich.

2.2. Protein purification

Choline-bound CbpF was purified and crystallized as described earlier [22], obtaining a protein final concentration of 2.7 mg/ml in 20 mM Tris–HCl pH 8.0 plus 140 mM choline chloride.

2.3. Evaluation of binding strength of choline and choline analogs to CbpF

A 120-microliter aliquot from a sonicated extract overproducing the CbpF protein [22] was incubated with 60 μl of fluidMAG DEAE-starch magnetic nanoparticles (200 nm diameter, approx. 5.5×10^{12} particles/ml) (Chemicell, Germany) for 15 min. These nanoparticles act as an affinity matrix for CbpF and other CBPs (manuscript in preparation). Non-bound proteins were separated by the application of an external magnet (Chemicell) and the particles were first washed with 1 M NaCl and then incubated with 120 μl of 20 mM sodium phosphate buffer, pH 7.0, containing the corresponding concentrations of choline or choline analogs. Due to the interference of atropine and ipratropium in the UV region, precluding quantification by absorption spectroscopy, the eluted protein was quantified using the Bio-Rad Protein Assay using hen egg-white lysozyme as the calibration standard.

2.4. Crystallization and data collection

Crystallization of CbpF in the presence of choline was accomplished as described [22]. In order to obtain complexes with drugs, two techniques were used: (i) fast soaking, in which the CbpF crystals were transferred for 10 s to a drop of reservoir solution with ipratropium at 500 mM and (ii) co-crystallization, in which the protein solution was incubated overnight with 10 mM of atropine, and then mixed with the reservoir solution. The reservoir solutions contained 0.2 M ammonium sulphate, 30% PEG 8000 and 0.1 M sodium cacodylate buffer pH 6.5. Crystals up to $0.7 \times 0.4 \times 0.3$ mm were grown in one week. Crystals were cryoprotected by a quick soak in reservoir solution containing 15% (v/v) glycerol and flash-cooled in liquid nitrogen, maintained at 100 K during data collection. CbpF:ipratropium complex was measured on an ADSC Quantum 210 image plate detector at beamline BM16 of the ESRF (European Synchrotron Radiation Facility, Grenoble, France). CbpF:atropine complex was measured on a MAR 345 image-plate detector using Cu Kα X-Rays generated by an in-house Enraf-Nonius rotating-anode generator equipped with a double-mirror focusing system and operated at 40 kV and 90 mA. All data sets collected at ESRF were processed using *XDS* [23] and scaled with *SCALA* from the *CCP4* package [24]. Data set collected with Cu Kα radiation was integrated using *MOSFLM* [25] and scaled with *SCALA*. A summary of data-collection parameters and processing statistics is shown in Table 1.

2.5. Structure determination and refinement

The three-dimensional structure of CbpF complexes was solved by the molecular replacement method with *MOLREP* program [26] from the CCP4 package. The CbpF native structure from *S. pneumoniae* (PDB

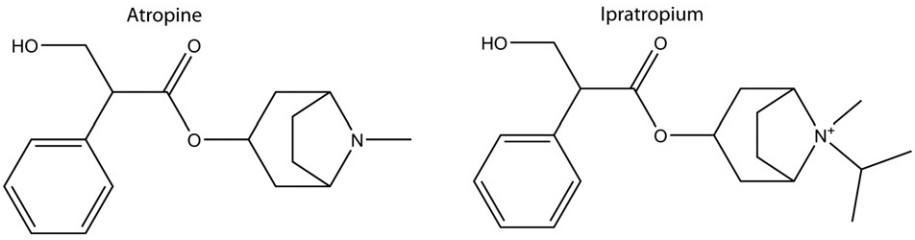

Fig. 1. A 2D representation of atropine and ipratropium, the esters of bicyclic amines used in the complex with CbpF. Drawings were rendered with ChemDraw 10.0 (CambridgeSoft).

Table 1
Data collections and refinement statistics for CbpF drug complexes.

	CbpF–ipratropium	CbpF–atropine
Data collection		
Space group	P 2_12_12	P 2_12_12
Cell dimensions *a*, *b*, *c* (Å)	52.33, 115.69, 73.20	52.54, 116.08, 73.17
Wavelength (Å)	0.9792	1.5418
T (K)	100	120
Resolution (Å)	57.84–1.85 (1.95)	31.16–2.03 (2.14)
R_{merge}[a]	0.093 (0.570)	0.129 (0.646)
R_{pim}[b]	0.038 (0.385)	0.056 (0.357)
Mean ((I)/σ (I))	14.3 (2.0)	6.1 (2.3)
No. of total reflections	269,402	348,949
No. of unique reflections	38,655	29,124
Completeness (%)	99.7 (97.9)	77.5 (77.5)
Redundancy	7.0 (5.8)	1.8 (1.8)
Refinement statistics		
Resolution range (Å)	47.68–1.85	24.73–2.27
No. of reflections	1936	1154
R_{work}/R_{free}[c]	0.219/0.256	0.226/0.288
Number of atoms		
Protein	2581	2581
Ligand (CHT + GOL + SO_4)	83	52
Drug	72	42
Water	403	286
R.m.s. deviations		
Bond length (Å)	0.009	0.007
Bond angles (°)	2.5	2.1
Average B-factor (Å^2)	31.7	28.5

Values in parentheses correspond to the highest resolution shell.
[a] $Rsym = \Sigma|I - I_{av}| / \Sigma I$, where the summation is over symmetry equivalent reflections.
[b] R_{pim}, precision-indicating (multiplicity-weighted) R_{merge}.
[c] R_{free} value calculated for 5% of data excluded from the refinement.

ID: 2V04) was used as initial model. Atropine and ipratropium molecules were modeled with "The Dundee PRODRG2 Server" (http://davapc1.bioch.dundee.ac.uk/prodrg/) [27] to generate initial coordinates. The models were subjected to successive refinement cycles with the CNS program [28] and intensive manual model building used the software package O [8]. Excellent density maps were obtained for CbpF complex structure. Water molecules were gradually added with waterpick routine of CNS program. Refinement of these structures was carried out with the PHENIX program [29]. The final models presented good stereochemistry parameters and *R* and R_{free} values (Table 1). Figures were rendered using the software package PyMOL (Delano Scientific LLC). Solvent accessible surface area (ASA) calculations on the resulting structures were carried out using the utilities provided by the Center for Informational Biology (Ohanomizu University, Tokyo, Japan) (http://cib.cf.ocha.ac.jp/bitool/ASA/), using a 1.4 Å radius probe for water. To calculate the accessible area buried only by the bicyclic moiety of atropine and ipratropium, a modified PDB file was created with the 3D coordinates of the atoms belonging to the tropic acid moiety removed.

The atomic coordinates and structure factors of the CbpF:ipratropium complex (PDB ID: 2X8M) and CbpF:atropine complex (PDB ID: 2X8P) have been deposited in the Protein Data Bank, Research Collaboratory for Structural Bioinformatics, Rutgers University, New Brunswick, NJ (http://www.pdb.org/).

3. Results

3.1. Affinity of CbpF for EBAs

It has been previously demonstrated that EBAs show a higher binding affinity than choline for several CBPs, at least LytA, LytB, LytC and CbpE [21]. To check whether this was also the case for CbpF, we attempted the biophysical characterization of the binding of atropine and ipratropium to this protein by spectroscopic methods (circular dichroism, fluorescence). However, this approach turned out unfeasible due to the low solubility of CbpF upon removal of the choline used in its purification, preventing the availability of ligand-free protein. Therefore, we envisaged an alternative method based on that used previously to identify atropine and ipratropium as high affinity ligands for the C-LytA module [21]. CbpF was selectively immobilized in DEAE-functionalized magnetic nanoparticles by affinity chromatography, and these were then incubated with limiting concentrations of eluting agents. Table 2 shows that, both at 2 mM or 5 mM concentration, the eluting efficiency of EBAs was higher than that of choline, being ipratropium the most effective. This confirms the trend observed with the other four CBPs [21] and supports the use of CbpF as a model for studying the interaction between CBPs and EBAs.

3.2. Crystal structure of CbpF:atropine complex

CbpF has unique features compared to other CBPs, as it is assembled entirely by choline-binding repeats that are distributed into two well-defined modules [9] (Fig. 2). The amino-terminal module (residues 1–128) shows a disk-shape conformation. Notably, the repeats building this module (dp1–dp4) appreciably differ from the canonical choline-binding repeats by the presence of both additional amino acids and mutations on different positions of the consensus motif, and consequently, this domain is not able to bind choline. On the other hand, the carboxy-terminal module (residues 129–311) follows a superhelical fold previously found in other CBMs and is arranged into two regions referred to as CI and CII (Fig. 2). The CII domain presents five choline-binding repeats (p1–p5), whereas the CI domain presents two choline-binding repeats (dp5 and dp6) modified by amino acid insertions that define a linker region with the N-terminal domain [9]. In this structure, seven choline molecules have been located in the CBM between two consecutive hairpins [9].

Crystals of CbpF in complex with atropine were obtained by co-crystallization as described above. Two atropine molecules (Atro1 and Atro2) were localized in the structure. The Atro1 molecule is bound to the choline-binding site between dp6 and p1 repeats (Fig. 2), in which the aromatic cavity (Trp163, Trp181, Tyr202) binds the bicyclic moiety of the ligand by hydrophobic and cation–π interactions (Fig. 3A). Upon binding, the ligand nearly duplicates the burial of protein surface in the binding site as compared to choline (Table 3) without substantially disturbing the arrangement of the residue side chains observed in the CbpF:choline complex (Supp. Fig. S1), although the bicyclic moiety only buries a slightly higher area than choline. These features are repeated for all the EBA sites described in this work. On the other hand, binding of the tropic acid moiety involves the formation of H-bonds between the two oxygen atoms in the ester group of Atro1 with the N_ε of Trp181. The Asn228 and Lys227 residues establish a set of van der Waals and hydrogen bond interactions with the ligand. Finally, a slight movement of the side chains of Asn198, Tyr202 and Met210 with respect to the choline-bound protein is observed in order to increase the interaction with the ligand (Supp. Fig. S1). However, the most remarkable characteristic is the packing of the Trp181 indole side chain against the aromatic ring of Atro1, establishing a highly stabilizing π–π interaction with a dihedral angle between rings of 72°. This simultaneous interaction (with the bicyclic and aromatic moieties of the ligand) exerted by

Table 2
Ability of compounds to elute CbpF immobilized in DEAE–dextran magnetic nanoparticles.

Eluent (mM)	Eluted protein (%)		
	Choline	Atropine	Ipratropium
2	6	16	23
5	14	23	53

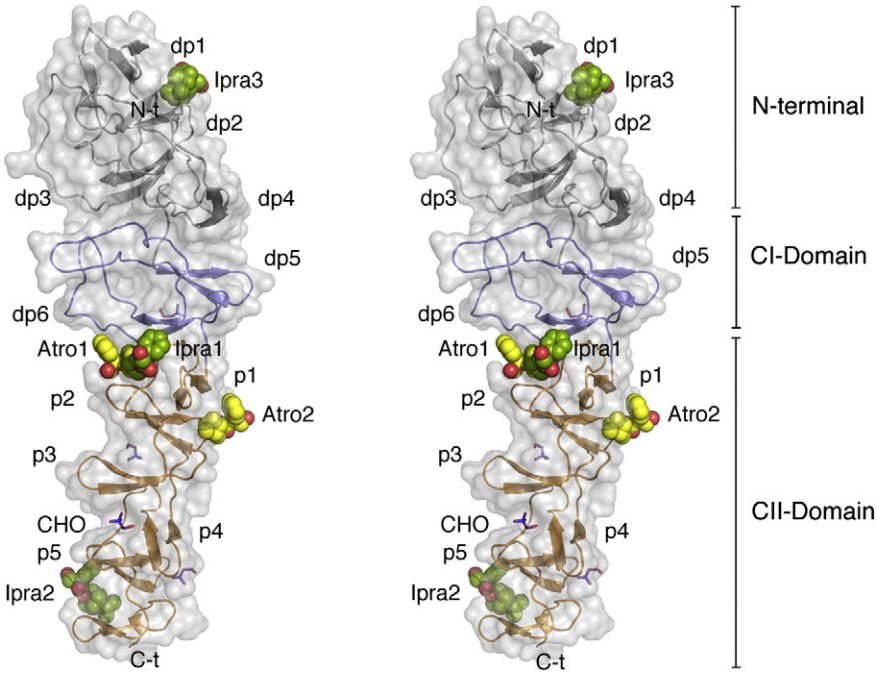

Fig. 2. Atropine and ipratropium ligands attached to pneumococcal CbpF. Stereoview representation of the general structure of CbpF in complex with atropine and ipratropium; complexes are superimposed to compare localization of both ligands. The atropine molecules are drawn as space-filled models in yellow and ipratropium molecules are drawn as space-filled models in green. The amino-terminal module of CbpF is in gray, the CI domain in blue and CII domain in orange. Choline molecules bound to the choline-binding sites are drawn as sticks. CbpF, choline-binding protein F. CHO, choline. p1–p5, canonical choline-binding repeats. dp1–dp6, non-canonical choline-binding repeats. Atro, atropine molecule. Ipra, ipratropium molecule.

the same aromatic side chain (Trp181 in this case) is repeated in all EBA binding sites (see below) and may explain the higher affinity shown by the CBPs for EBAs as compared to other choline analogs (including the corresponding non-sterified bicyclic amines) which was attributed to the presence of a suitably positioned aromatic group at a certain distance from the amine group [21]. Noteworthily, the hydroxyl group in atropine points towards the solvent and makes no interaction with the protein. This feature is also shared by the rest of EBA binding sites described in this work, and its relevance in the design of new EBA derivatives will be discussed below.

A second atropine molecule (Atro2) is located in the choline-binding site between the p1 and p2 repeats, introducing a slightly bigger distortion (Fig. 3B; Supp. Fig. S1). The bicyclic moiety is stabilized through cation–π interactions with Trp194, Trp201, and Tyr222, with additional van der Waals contributions from Met231 and Ser248. Again, a nearly perpendicular π–π interaction (115°) between the indole ring of the mentioned Trp201 and the tropic acid ring is established, which is further stabilized by van der Waals interactions with Lys196.

3.3. Crystal structure of CbpF:ipratropium complex

CbpF–ipratropium complexes were obtained by crystal soaking. Three ipratropium molecules were found attached to CbpF (Fig. 2). Two of them (Ipra1 and Ipra2) are located at two canonical choline-binding sites of the CBM replacing choline molecules, whereas, remarkably, the third molecule (Ipra3) is found in the N-terminal, non-choline-binding module. The Ipra1 binding site is the same as Atro1, with the additional van der Waals contribution of S_δ from Met210 (Fig. 4A; Supp. Fig. S1), and the increase in buried surface also follows the same trend (Table 3). With respect to the tropic acid moiety, here the amount of area buried by the bicycle is relatively higher than in the atropine case (Table 3). Moreover, the NH_2 side group of Asn198 establishes an H-bond interaction with the O-carbonyl in the ipratropium ester. Contrary to Atro1, in this case, the dual role of simultaneous interaction with the bicycle and the tropic acid moieties is performed by the other tryptophanyl group in the cavity (Trp163).

The second ipratropium molecule (Ipra2) is located in the choline-binding site between the p5 repeat and the C-terminal tail of the CBM. The most important feature of this site is the presence of a hydrophobic pocket conformed by four aromatic residues (Trp276, Trp283, Tyr301 and Trp309), in which the ipratropium isopropyl group is buried mimicking choline interactions (Fig. 4B). A 3.4 Å-long H-bond between the N_ε of Trp276 and the O-carbonyl group in Ipra2 is observed. Again, a nearly perpendicular stacking of the aromatic rings of the ligand and the side chain of Trp283 takes place confirming the role of the tropic acid moiety in the interaction. The binding site is here more appreciably distorted by the bicyclic moiety of ipratropium (Supp. Fig. S1), which induces a slight displacement of the Trp309 indole ring and also of Tyr301 side chain compared to the choline situation.

Strikingly, Ipra3 is located in the N-terminal module, bound in a pocket between dp1 and dp2 repeats, for which no interaction with choline was previously reported (Fig. 4C). While the bicyclic moiety is well defined in the electron-density map, the tropic acid part is more disordered and therefore conclusions involving it should be taken cautiously. In this site, the entrance of ipratropium does not either appreciably perturb the disposition of the side chains involved in binding and their immediate surroundings (Supp. Fig. S1). The choline-mimicking bicyclic part is stabilized by hydrophobic and cation–π interactions with Phe7 and Tyr34, and displays van der Waals contacts with the side chains of Lys14, Met42 and Asp81, which in turn is suitably positioned to establish an ionic bond with the quaternary amine. The fact that only two aromatic rings are well positioned to interact with the amine through cation–π forces instead of the usual three, and the relatively long distance of Lys14 and Met42 from the small methyl groups in choline, creates a cavity of a bigger size than the canonical choline-binding sites, allowing in fact the accommodation of a voluminous ipratropium molecule (Table 3). This may explain why choline is not found in this site, as it would be too small to fit. Furthermore, the additional interactions supplied by the tropic acid ring in ipratropium must also contribute decisively to its binding. These interactions include a π–π interaction with Tyr34, van der Waals contacts with Phe7 and Lys32 and, additionally, a hydrogen bond between the N_ε group of the latter residue and the OH group in the ligand.

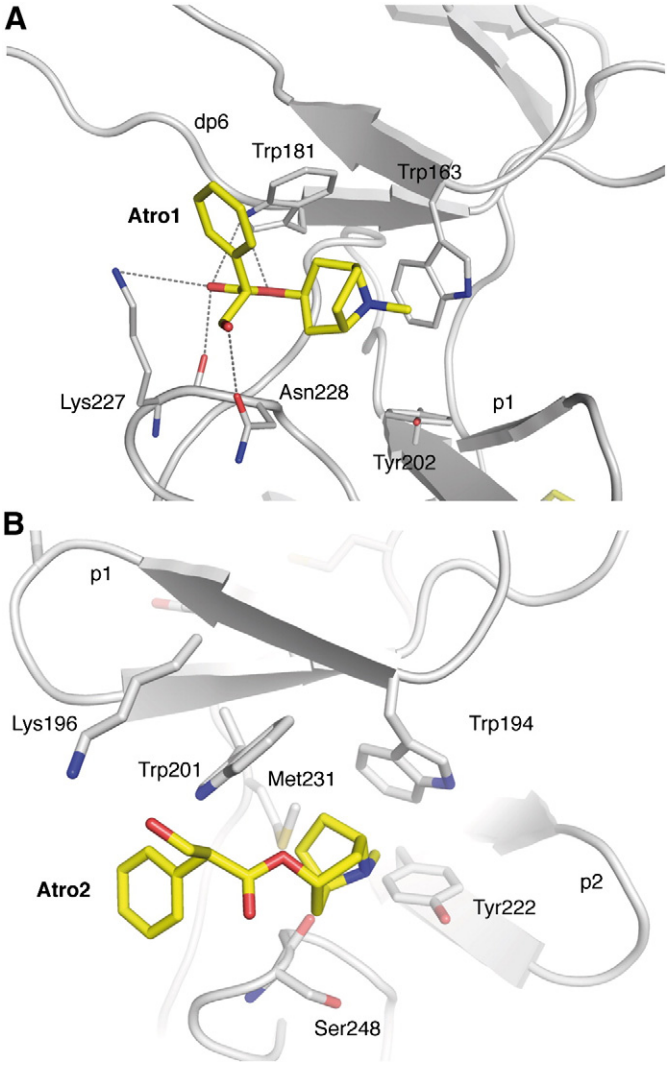

Fig. 3. Details of the atropine recognition by CbpF. The views show the interactions between CbpF and atropine. The residues forming the binding site are drawn as capped sticks. Carbon atoms of the ligand are in yellow. Hydrogen bonds are shown as dashed lines. (A) Atropine recognition at the cavity between dp6 and p1 repeats. (B) Atropine recognition at the cavity between p1 and p2 repeats.

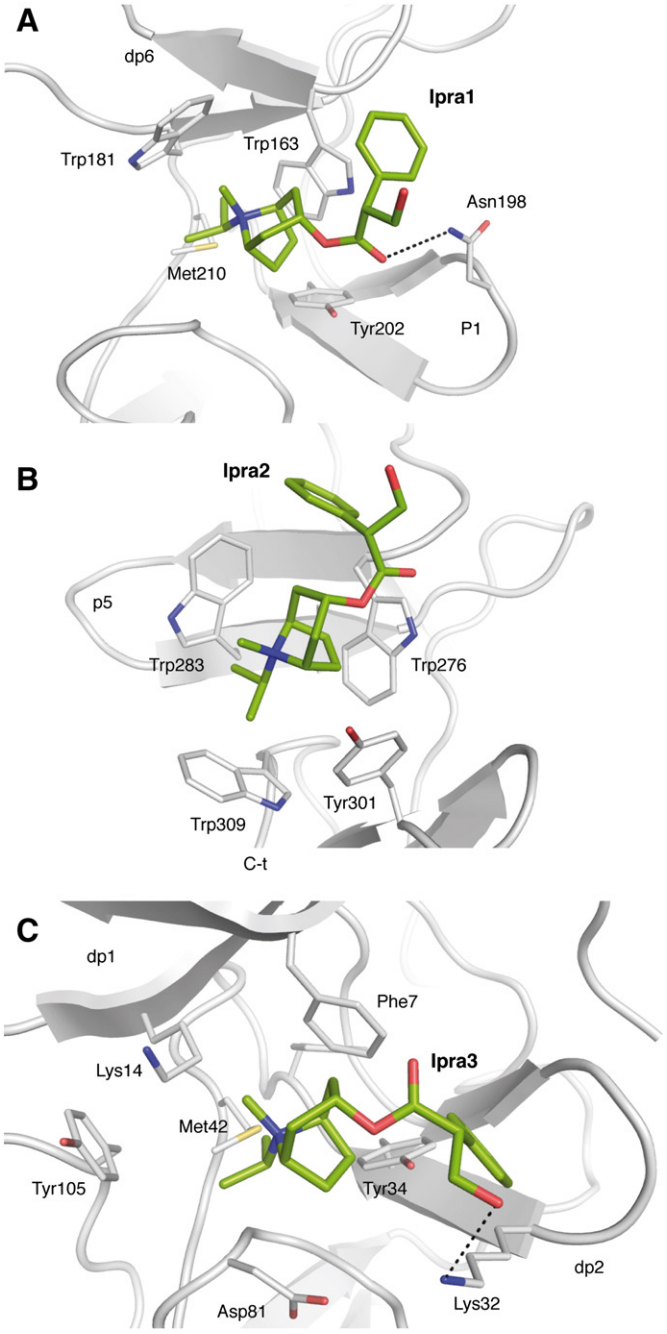

Fig. 4. Details of the ipratropium recognition by CbpF. The views show the interactions between CbpF and ipratropium. The residues forming the binding site are drawn as capped sticks. Carbon atoms of the ligand are in green. Hydrogen bonds are shown as dashed lines. (A) Ipratropium recognition at the cavity between dp6 and p1 repeats. (B) Ipratropium recognition at the cavity between p5 and the C-terminal. (C) Ipratropium recognition at the cavity between dp1 and dp2 repeats.

4. Discussion

The differential effects shown by atropine and ipratropium on CBP inhibition, arrest of growth and bactericidal rate, when compared to choline [21], are, *a priori*, somehow unexpected. First, it has long been demonstrated that CBPs may accommodate a high number of tertiary and quaternary alkyl amines in their choline-binding sites [15,16,21,30], even bulky ones and including bicycles such as tropine, the amine part of atropine, as well as quinuclidine and pseudopelletierine [21], all of them with similar affinities compared to choline. Since atropine and ipratropium are appreciably better binders to C-LytA than tropine and differ from the latter mainly in the presence of the tropic acid moiety, the higher affinity displayed by these EBAs was ascribed to their aromatic ring. However, specific, stringent structural constraints should also take place in the EBA–CBP interaction because the mere presence of aromatic rings in choline analogs is not sufficient to turn an alkyl amine into a high-affinity CBP ligand [*e.g.* benzoyl-choline or 3-(dimethylamino)propiophenone] [21]. Moreover, while inhibition of CBPs by choline and other analogs is manifested in *in vitro* bacterial cultures as the formation of long chains

Table 3
Accessible surface area characteristics of the atropine- and ipratropium-binding sites in CbpF.

EBA ligand	Buried surface by ligand (Å^2)	Buried surface by bicyclic moiety of the ligand (Å^2)	Buried surface by corresponding choline (Å^2)
Atro1	220	129	114
Atro2	198	114	99
Ipra1	207	168	114
Ipra2	189	134	105
Ipra3	182	112	–

resulting from the lack of cell separation upon division [15,18], EBAs induce in turn appreciable morphological deformations, growth arrest and reduced cell viability [21].

The analysis of CbpF–EBA complexes contributes to a better understanding of the structural features of the interactions of CBPs with these ligands. Due to the difficulties in maintaining enough CbpF in choline-free solutions, our crystallization experiments were performed in all cases in the presence of 140 mM choline. However, even under these conditions, EBA molecules displaced the CbpF-bound choline molecules (Supp. Fig. S1). It is therefore expected that more EBA-binding sites would be available in the absence of pre-bound choline molecules. Besides, the lack of significant distortion in the binding sites upon EBA recognition (compared to choline binding) (Supp. Fig. S1) is an entropically favored event that the better binding of these ligands. The bicycle moieties are involved in hydrophobic and cation–π interactions with the protein, and are responsible of the burial of approximately only 25% more surface than choline on average (Table 3) although, as mentioned above for the atropine case, this is not sufficient to account for the much higher affinity of EBAs [21] (Table 2). The major determinant in the EBA–CbpF enhanced interaction seems to involve the additional π–π interaction between one of the amine-binding aromatic side chains and the tropic acid moiety in the EBAs. The particular geometry of atropine and ipratropium in the binding site configures a spatial disposition that is very adequate for the insertion of an aromatic side chain which establishes two simultaneous, highly stabilizing interactions with the ligand. Further developments of EBA analogs as CBP inhibitors should contemplate the conservation or optimization of this aromatic–aromatic interaction by the judicious positioning of the aromatic ring. In order to evaluate the possible generalization of these binding characteristics to the rest of the CBPs, a comparison of the EBA-binding sites in CbpF with the previously reported structures of other CBPs (LytA, LytC, CbpE, Spr1274 and Cpl-1) was performed (Supp. Figs. S3 and S4). The three types of ipratropium interaction found in the CbpF:ipratropium complex are present among all the known three-dimensional structures of CBPs (Supp. Fig. S3). The Ipra-1 and Ipra-3 binding sites are more abundant in LytC (4 sites) and in CbpE (3 sites) respectively. Ipra-2 binding sites are equally available in CbpE and LytC (3 sites each). Other CBPs such as LytA present just one ipratropium binding-site similar to that found for Ipra2, Spr1274 presents two sites (one for Ipra1 and one for Ipra2) and the phage-encoded endolysin Cpl-1 presents three (one for Ipra-1 and two for Ipra3). Two types of interaction were found for atropine in the CbpF:atropine complex (Supp. Fig. S4). While Atro-2 binding site is mainly stabilized by cation–π interactions with the aromatic residues conforming to the canonical choline-binding site, the Atro-1 binding site presents more polar interactions with Asn, Lys and Trp residues (Fig. 3A). This Atro-1 binding site was found just in CbpE (two sites) and Spr1274 (one site) but not in other structurally known CBPs. In summary, our analysis reveal that EBA binding-sites are distributed among all known structures of CBPs (Supp. Fig. S5), in accordance with our previous results that demonstrated a wide range of CBPs affected by these compounds [21], so that they may represent a universal set of CBP inhibitors.

On the other hand, the protein surface buried by atropine and ipratropium is similar (Table 3), despite the presence of an additional isopropyl group as N-substituent in ipratropium (Fig. 1), so that the higher affinity shown by the latter [21] (Table 2) should be better ascribed to its permanent positive charge, which reinforces the cation–π component in the interaction. Moreover, most of the EBA–CbpF interactions leave the OH group in the ligand unbonded and pointing towards the solvent. It should be remarked that this OH has been termed as essential for a productive interaction of atropine and ipratropium with the muscarinic acetylcholine receptors [31,32]. Therefore, it is likely that the removal of the dispensable aliphatic OH group would render new EBA analogs with the same affinity for CBPs but with a decrease side-effect on muscarinic receptors. This should also be taken into account when designing novel EBA-based antimicrobials.

To date, the bactericidal effect of EBA molecules on pneumococcal cultures has not been assigned to a particular surface CBP. While this is investigated, the specific binding of EBAs to CbpF may be very interesting in itself and not only as a general model of EBA–CBP interactions. The methodological limitations associated to the obtention of crystals cannot rule out the possibility of binding of more molecules of ipratropium and atropine when the protein is in the presence of these compounds both *in vitro* and *in vivo*. In our study, the most striking feature is the presence of an ipratropium molecule in the N-terminal, non-choline-binding domain of the protein. It has been described that CbpF *in vivo* can not only inhibit the lysozyme activity of pneumococcal autolysin LytC, but also regulate other pneumococcal phage lysozymes such as Cpl-1 or Cpl-7 [22]. CbpF regulation of LytC is relevant due to the role of this autolysin in both the colonization of the nasopharynx [33] and in the virulence mechanism of "fratricide" process, in which competent pneumococci lyse and kill non-competent pneumococcal sister cells, as well as other bacteria from closely related species [34,35]. Due to the presumed lack of functional features in the C-terminal domain of the protein other than binding to choline-containing teichoic acids, it is tempting to speculate that relevant CbpF interactions take part through the N-terminal domain. In fact, the isolated N-terminal moiety of CbpF has been demonstrated to bind pneumococcal cell wall without choline [11], so that N- and C-terminal modules of CbpF bind to different components of peptidoglycan. Moreover, recognition of host elastin and plasminogen by CbpF has also been recently reported [8]. On this basis, other CbpF–protein interactions might as well be modulated by ipratropium. Whether ipratropium is able to influence pneumococcal fratricide through binding to CbpF is also a subject that deserves further investigation.

In summary, our results provide an explanation to the fact that EBAs are better CBP binders than choline and confirm the importance of the presence of an aromatic group specifically located with a determined geometry in the ligand. Furthermore, it is reasonable to think that the design of new EBA analogs specifically optimized for the binding to the N-terminal moiety of CbpF, besides to the canonical choline-binding sites, might influence the interaction of CbpF with its cognate proteins, opening up a new research line for the synthesis of successful antipneumococcal drugs.

Acknowledgements

We thank D. Bello, J. Pupo, H. de Paz, M. Garzón, M. Gutiérrez, C. Fuster and J. Casanova for their excellent technical assistance. Noella Silva-Martín was a fellow of the Fundayacucho Foundation (Venezuela). This work was supported by grants BIO2007-67304-C02-02, BFU2010-17824 and BFU2011-25326 (Spanish Ministry of Education and Science), EU-CP223111 (CAREPNEUMO, European Union) and from Madrid Regional Government (S2010/BMD-2457).

Appendix A. Supplementary data

Supplementary data to this article can be found online at http://dx.doi.org/10.1016/j.bbagen.2013.09.006.

References

[1] B. Maestro, J.M. Sanz, Novel approaches to fight *Streptococcus pneumoniae*, Recent Pat. Antiinfect. Drug Discov. 2 (2007) 188–196.
[2] Weekly Epidemiol, vol. 82, World Health Organization, 2007, pp. 93–104.
[3] K.L. O'Brien, L.J. Wolfson, J.P. Watt, E. Henkle, M. Deloria-Knoll, N. McCall, E. Lee, K. Mulholland, O.S. Levine, T. Cherian, T. Hib, Pneumococcal Global Burden of Disease Study, Burden of disease caused by *Streptococcus pneumoniae* in children younger than 5 years: global estimates, Lancet 374 (2009) 893–902.
[4] A. Tomasz, Choline in the cell wall of a bacterium: novel type of polymer-linked choline in *Pneumococcus*, Science 157 (1967) 694–697.
[5] S. Janecek, B. Svensson, R.R. Russell, Location of repeat elements in glucansucrases of *Leuconostoc* and *Streptococcus* species, FEMS Microbiol. Lett. 192 (2000) 53–57.
[6] S. Bergmann, S. Hammerschmidt, Versatility of pneumococcal surface proteins, Microbiology 152 (2006) 295–303.

[7] R. Hakenbeck, A. Madhour, D. Denapaite, R. Bruckner, Versatility of choline metabolism and choline-binding proteins in *Streptococcus pneumoniae* and commensal streptococci, FEMS Microbiol. Rev. 33 (2009) 572–586.
[8] C. Frolet, M. Beniazza, L. Roux, B. Gallet, M. Noirclerc-Savoye, T. Vernet, A.M. Di Guilmi, New adhesin functions of surface-exposed pneumococcal proteins, BMC Microbiol. 10 (2010) 190.
[9] J.A. Hermoso, B. Monterroso, A. Albert, B. Galan, O. Ahrazem, P. Garcia, M. Martinez-Ripoll, J.L. Garcia, M. Menendez, Structural basis for selective recognition of pneumococcal cell wall by modular endolysin from phage Cp-1, Structure 11 (2003) 1239–1249.
[10] J.A. Hermoso, L. Lagartera, A. Gonzalez, M. Stelter, P. Garcia, M. Martinez-Ripoll, J.L. Garcia, M. Menendez, Insights into pneumococcal pathogenesis from the crystal structure of the modular teichoic acid phosphorylcholine esterase Pce, Nat. Struct. Mol. Biol. 12 (2005) 533–538.
[11] R. Molina, A. Gonzalez, M. Stelter, I. Perez-Dorado, R. Kahn, M. Morales, M. Moscoso, S. Campuzano, N.E. Campillo, S. Mobashery, J.L. Garcia, P. Garcia, J.A. Hermoso, Crystal structure of CbpF, a bifunctional choline-binding protein and autolysis regulator from *Streptococcus pneumoniae*, EMBO Rep. 10 (2009) 246–251.
[12] I. Perez-Dorado, A. Gonzalez, M. Morales, R. Sanles, W. Striker, W. Vollmer, S. Mobashery, J.L. Garcia, M. Martinez-Ripoll, P. Garcia, J.A. Hermoso, Insights into pneumococcal fratricide from the crystal structures of the modular killing factor LytC, Nat. Struct. Mol. Biol. 17 (2010) 576–581.
[13] C. Fernandez-Tornero, R. Lopez, E. Garcia, G. Gimenez-Gallego, A. Romero, A novel solenoid fold in the cell wall anchoring domain of the pneumococcal virulence factor LytA, Nat. Struct. Biol. 8 (2001) 1020–1024.
[14] Z. Zhang, W. Li, C. Frolet, R. Bao, A.M. di Guilmi, T. Vernet, Y. Chen, Structure of the choline-binding domain of Spr1274 in *Streptococcus pneumoniae*, Acta Crystallogr. Sect. F Struct. Biol. Cryst. Commun. 65 (2009) 757–761.
[15] J.M. Sanz, R. Lopez, J.L. Garcia, Structural requirements of choline derivatives for 'conversion' of pneumococcal amidase. A new single-step procedure for purification of this autolysin, FEBS Lett. 232 (1988) 308–312.
[16] J.M. Sanchez-Puelles, J.M. Sanz, J.L. Garcia, E. Garcia, Immobilization and single-step purification of fusion proteins using DEAE-cellulose, Eur. J. Biochem./FEBS 203 (1992) 153–159.
[17] B. Maestro, I. Velasco, I. Castillejo, M. Arevalo-Rodriguez, A. Cebolla, J.M. Sanz, Affinity partitioning of proteins tagged with choline-binding modules in aqueous two-phase systems, J. Chromatogr. A 1208 (2008) 189–196.
[18] T. Briese, R. Hakenbeck, Interaction of the pneumococcal amidase with lipoteichoic acid and choline, Eur. J. Biochem./FEBS 146 (1985) 417–427.
[19] C. Fernandez-Tornero, E. Garcia, B. de Pascual-Teresa, R. Lopez, G. Gimenez-Gallego, A. Romero, Ofloxacin-like antibiotics inhibit pneumococcal cell wall-degrading virulence factors, J. Biol. Chem. 280 (2005) 19948–19957.
[20] V.M. Hernandez-Rocamora, B. Maestro, B. de Waal, M. Morales, P. Garcia, E.W. Meijer, M. Merkx, J.M. Sanz, Multivalent choline dendrimers as potent inhibitors of pneumococcal cell-wall hydrolysis, Angew. Chem. 48 (2009) 948–951.
[21] B. Maestro, A. Gonzalez, P. Garcia, J.M. Sanz, Inhibition of pneumococcal choline-binding proteins and cell growth by esters of bicyclic amines, FEBS J. 274 (2007) 364–376.
[22] R. Molina, A. Gonzalez, M. Moscoso, P. Garcia, M. Stelter, R. Kahn, J.A. Hermoso, Crystallization and preliminary X-ray diffraction studies of choline-binding protein F from *Streptococcus pneumoniae*, Acta Crystallogr. Sect. F Struct. Biol. Cryst. Commun. 63 (2007) 742–745.
[23] W. Kabsch, XDS, Acta Crystallogr. D Biol. Crystallogr. 66 (2010) 125–132.
[24] N. Collaborative Computational Project, The CCP4 suite: programs for protein crystallography, Acta Crystallogr. D Biol. Crystallogr. 50 (1994) 760–763.
[25] A.G.W. Leslie, Crystallographic Computing 5: From Chemistry to Biology, Oxford University Press, 1992.
[26] G.N. Murshudov, A.A. Vagin, E.J. Dodson, Refinement of macromolecular structures by the maximum-likelihood method, Acta Crystallogr. D Biol. Crystallogr. 53 (1997) 240–255.
[27] A.W. Schuttelkopf, D.M. van Aalten, PRODRG: a tool for high-throughput crystallography of protein–ligand complexes, Acta Crystallogr. D Biol. Crystallogr. 60 (2004) 1355–1363.
[28] A.T. Brunger, P.D. Adams, G.M. Clore, W.L. DeLano, P. Gros, R.W. Grosse-Kunstleve, J.S. Jiang, J. Kuszewski, M. Nilges, N.S. Pannu, R.J. Read, L.M. Rice, T. Simonson, G.L. Warren, Crystallography & NMR system: a new software suite for macromolecular structure determination, Acta Crystallogr. D Biol. Crystallogr. 54 (1998) 905–921.
[29] P.D. Adams, P.V. Afonine, G. Bunkoczi, V.B. Chen, I.W. Davis, N. Echols, J.J. Headd, L.W. Hung, G.J. Kapral, R.W. Grosse-Kunstleve, A.J. McCoy, N.W. Moriarty, R. Oeffner, R.J. Read, D.C. Richardson, J.S. Richardson, T.C. Terwilliger, P.H. Zwart, PHENIX: a comprehensive Python-based system for macromolecular structure solution, Acta Crystallogr. D Biol. Crystallogr. 66 (2010) 213–221.
[30] B. Maestro, C.M. Santiveri, M.A. Jimenez, J.M. Sanz, Structural autonomy of a beta-hairpin peptide derived from the pneumococcal choline-binding protein LytA, Protein Eng. Des. Sel. 24 (2011) 113–122.
[31] A.R. Cushny, On optical isomers VIII. The influence of configuration on the activity of tropeines, J. Pharmacol. Exp. Ther. 29 (1926) 5–16.
[32] R.B. Barlow, S. Ramtoola, The size of the hydroxyl group and its contribution to the affinity of atropine for muscarine-sensitive acetylcholine receptors, Br. J. Pharmacol. 71 (1980) 31–34.
[33] K.K. Gosink, E.R. Mann, C. Guglielmo, E.I. Tuomanen, H.R. Masure, Role of novel choline binding proteins in virulence of *Streptococcus pneumoniae*, Infect. Immun. 68 (2000) 5690–5695.
[34] O. Johnsborg, V. Eldholm, M.L. Bjornstad, L.S. Havarstein, A predatory mechanism dramatically increases the efficiency of lateral gene transfer in *Streptococcus pneumoniae* and related commensal species, Mol. Microbiol. 69 (2008) 245–253.
[35] J.P. Claverys, L.S. Havarstein, Cannibalism and fratricide: mechanisms and raisons d'etre, Nat. Rev. Microbiol. 5 (2007) 219–229.